Exploring the Electronic Properties of Extended Benzofuran-Cyanovinyl Derivatives Obtained from Lignocellulosic and Carbohydrate Platforms Raw Materials

Nagham Ibrahim,[a] Chady Moussallem,[b] Magali Allain,[a] Olivier Segut,[a] Frédéric Gohier,[a] and Pierre Frère*[a]

Two series of linear extended benzofuran derivatives associating cyanovinyl unit and phenyl or furan moieties obtained from benzaldehyde-lignocellulosic (**Be** series) or furaldehyde –saccharide (**Fu** series) platforms were prepared in order to investigate their emission and electrochemical properties. For the fluorescence in solution and solid states, contrasting results between the two series were demonstrated. For **Be** series a net aggregation induced emission effect was observed with high fluorescence quantum yield for the solid state. A [2 + 2] cycloaddition under irradiation at 350 nm was also revealed for one derivative of **Be** series. In contrast, for **Fu** series the fluorescence in solution is higher than in the solid state. The X-ray crystallography studies for the compounds reveal the formation of strong π-π stacking for the derivatives without emissive property in the solid state and the presence of essentially lateral contacts for emissive compounds. Taking advantage of the propensity to develop 2D π-stacking mode for the more extended derivative with a central furan cycle, organic field effect transistors presenting hole mobility have been made.

Introduction

The organic semiconductors (OSC) based on π-conjugated systems have seen increasing interest in recent years as an alternative to inorganic optoelectronic devices for the development of new generation of organic photovoltaic cells (OPV) for clean energy production, organic electroluminescent diodes (OLED) for more energy-efficient lighting and display systems and transistor-type electronic devices (OFETs). The most conjugated systems are synthesized from substrates of petroleum origin. Utilization of biomass as raw materials to produce the conjugated structure of OSC can liberate from the reliance on fossil resource and so allow the development of renewable materials. Although polyfunctional conjugated synthons, derived from lignocellulosic biomass,[1,2,3,4] represent potential raw materials for the development of OSC materials, alternatives for using these bio-sourced molecules have so far been rarely developed.[5,6] Lignin is a very important sustainable feedstock strongly worked for the development of methoxy-benzaldehyde derivatives such as vanillin and syringaldehyde.[7,8,9,10] On the other hand, many works are also devoted to the access of furaldehyde derivatives such as 5-hydroxymethylfurfural (HMF) from biomass derived carbohydrates for the development of new generation of biofuels or as renewable raw materials for chemistry in pharmaceutical or materials chemistry.[11,12,13,14] Over the last decade, works about furan-based conjugated derivatives brought out relevant benefits of the furan cycle for the development of semi-conducting materials for optoelectronic devices.[15,16,17,18] The insertion of low aromaticity cycle such as furan into a conjugated chain allows to increase the rigidity and the planarity of the structure and thus to enhance the electronic delocalization along the conjugated systems.[18,19] Benzofuran represents also a privileged heterocyclic framework with extensive applications in medicinal chemistry and material sciences. Benzofuran based semiconductors have been investigated in OFET and solar cell devices.[20,21,22] Moreover, linear extended benzofuran derivatives are efficient luminophores presenting high quantum yield both in solution and in the solid state.[23,24]

In the continuation of our current interest in conjugated systems based on benzofuran units, we have prepared and explored the electronic properties of two new series of derivatives associating benzofuran-cyanovinyl unit with phenyl or furan moieties obtained from benzaldehyde-lignocellulosic (**Be1**–**Be3**) or furaldehyde –saccharide (**Fu1**–**Fu2**) platforms (Figure 1).

Results and Discussion

The target molecules were easily synthesized by Knoevenagel condensations between the benzofuran acetonitrile derivative **1** (Figure 1) and the corresponding benzaldehyde or furaldehyde derivatives obtained from the biomass platforms. 3,4-dimethoxybenzaldehyde and 3,4,5-trimethoxybenzaldehyde were

[a] N. Ibrahim, M. Allain, Dr. O. Segut, Dr. F. Gohier, Prof. P. Frère
Univ Angers
CNRS UMR 6200, MOLTECH-ANJOU,SFRMATRIX
2 boulevard Lavoisier, 49000 Angers (France)
E-mail: pierre.frere@univ-angers.fr
[b] Dr. C. Moussallem
Université Libanaise
Faculté des Sciences
Laboratoire de Chimie
Campus Michael Slayman, Maska 1352 (Lebanon)

Supporting information for this article is available on the WWW under https://doi.org/10.1002/cplu.202100062

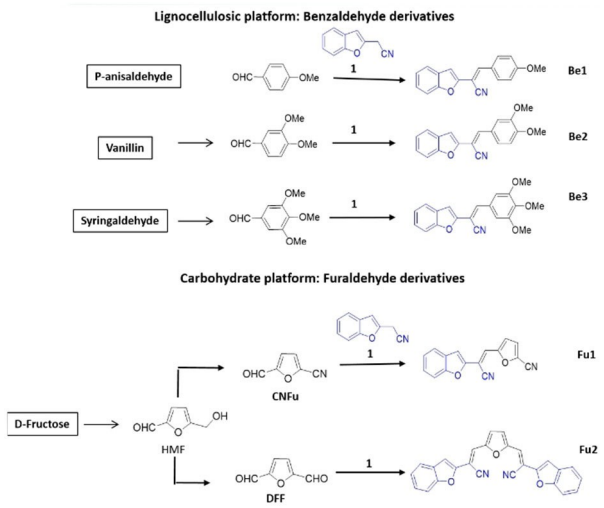

Figure 1. Molecular structures of compounds **Be1**–**Be3** and **Fu1**–**Fu2** associating benzofuran unit with phenyl and furan moieties issued from biosourced benzaldehyde or furaldehyde derivatives

easily obtained by Williamson reaction between vanillin or syringaldehyde and methyliodide or dimethylsulfate in acetone with potassium carbonate as base. Among the many methods to prepare HMF described in the literature,[25,26,27] we have opted for facile procedures from D-fructose employed by students in practical works (Scheme 1). The dehydration of D-fructose into HMF can be performed in ionic liquid (IL) such as 1-butyl-3-methyl imidazolium chloride in the presence of Amberlyst 15 as acid catalyst.[28,29] The reaction was performed from 0.3 g of fructose in 2 mL of IL with 150 mg of catalyst. After stirring at 60 °C during 20 min, HMF was extracted with ethyl acetate and directly used for the oxidation step without purification. The IL-catalyst system can be reused several times by adding 0.3 g of fructose at each cycle. The average yield in HMF obtained per cycle was about 30% even after ten cycles. A second efficient method consisted in the HCl-catalysed conversion of fructose by proceeding in isopropyl alcohol at 120 °C.[30] Larger quantity of HMF can be synthesized in 50% yield but a flash chromatography was necessary to use HMF in the next step.

HMF is converted to nitrile derivative **HMF-CN** in 70% yield by the direct conversion of aldehyde into nitrile by treatment with aqueous ammoniac at 30% followed by the addition of 1 equivalent of iodine. The reaction proceeds by the formation of the imine that is oxidized into nitrile by the iodine.[31,32]

The oxidations of HMF in diformyl-furan **DFF** and the nitrile derivatives into aldehyde **CNFu** were performed with oxygen in presence of two different catalytic systems. Firstly, the couple $VOSO_4$-$Cu(NO_3)_2$ as catalyst described by J. Ma et al.[33] used in 5% mol under pressure of 1 bar in pure oxygen at 80 °C in acetonitrile gave the aldehyde derivatives **DFF** and **CNFu** in 70% and 85% yield. A second catalytic systems, $FeNO_3$ and TEMPO as catalyst (5% mol) and $NaNO_2$ as additive in acetonitrile, recently described by Hong et al.[34] led to **DFF** and **CNFu** in 85% and 90% yield respectively.

2-Benzofuranacetonitrile **1** was obtained in two steps from 2-hydroxyphenylacetic acid by using microwave irradiations as shown in scheme 2. The 2-coumaranone was easily prepared in 90% yield by cyclisation of 2-hydrophenylacetic acid under microwave irradiation.[35,36] Then 2-benzofuran acetonitrile **1** was obtained by the condensation of the stabilized ylide **Y** on the 2-coumaranone.[23] Non classical Wittig reactions of lactones with stabilized ylides can be performed by using forcing conditions like high temperature and/or microwave irradiation..[37,38,39] The resulting ethylenic derivative is not isolated because undergoing tautomerism rearrangement to afford **1**.[40] The reaction proceeds rapidly in 15 min under microwave activation at 120 °C in toluene. After evaporation of toluene the residue was treated with methanol for separating the insoluble part of oxide of triphenylphosphine and compound **1**. This last is purified by flash chromatography on silica gel to give pure **1** in 77% yield. The oxide of triphenylphosphine recovered in 70% yield by the treatment with methanol, can be reduced by phenylsilane to give back triphenylphosphine.[41] This one can be reused to produce the stabilized **Y** by reaction with bromoacetonitrile in acetone followed by washing with an aqueous solution of sodium hydroxide. Thus about 60% of the phosphorus agent used for the Wittig reaction can be recycled.

X-ray structure of molecule **1** reveals the presence of the benzofuran moiety substituted in the 2-position by a cyanomethyl group (Figure S1 in the Supporting Information), thus confirming the prototropic reaction allowing to perform the aromatization of the furan unit.

Finally, the target molecules were synthesized by Knoevenagel reactions between the aldehydes and acetonitrile derivative **1** carried out in ethanol at room temperature in presence of catalytic amount of tBuONa. The obtained precipitates were filtered and washed with ethanol to give the compounds in range of 55–70% yields. The ^{1}H NMR of all the compounds in $CDCl_3$ are characterized by the presence of only one singlet corresponding to the signal of the vinylic proton and also one signal for the furanic proton of the benzofuran core. Moreover,

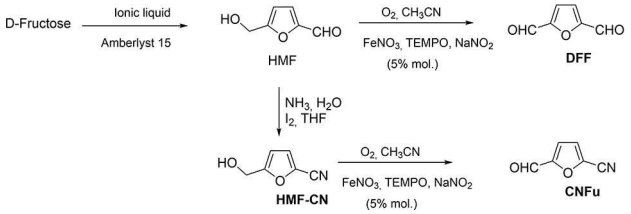

Scheme 1. Syntheses of **CNFu** and **DFF** from D-fructose.

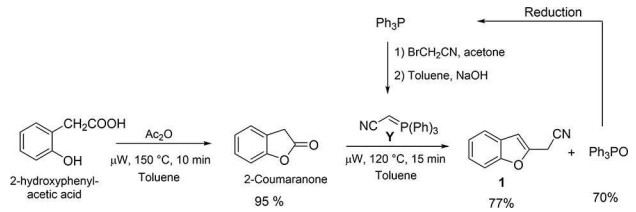

Scheme 2. Synthesis of benzofuran-acetonitrile **1**.

an exact number of carbons was observed in the ^{13}C NMR spectra of all the compounds. These NMR results provide sound evidence that only one configurational vinylene isomer (Z or E) has been isolated from the synthesized powders.

The X-ray structures of compounds **Be1**, **Be3**, **Fu1** and **Fu2** have been obtained from X-ray diffraction on single crystals obtained from slow evaporation of ethanol or chloroform-ethanol solutions. As shown in figure 2, **Be1**, **Be3** and **Fu1** present a E configuration of the cyanovinyl bonds and **Fu2** has a E–E configuration.

The crystal packing obtained from the diffraction studies are important to undertake for evaluating the roles of the cyano groups and the aromatic and heteroaromatic cycles in the intermolecular interactions. The electronic properties such as the emission in the solid state or the mobility of charge carriers in field effect transistors are strongly dependent on the stacking type of the molecules.

In **Be1** crystal, the molecules stack along the *a*-direction by forming head to tail π-dimers characterized by π-π interactions with many short interatomic distances inferior at 3.6 Å involving atoms of ethylenic bond and benzodifuran and phenyl units (blue dotted lines in figure 3A). In the columns, the dimers present π-interactions (green dotted lines in figure 3A) but there is not any short contact between adjacent columns. By contrast crystal **Be3** presents columns of molecules obtained by the direct superposition of the molecules (figure 3B). The nitrogen atoms of the cyano groups undergo in hydrogen bonds with hydrogen of methoxy groups (orange dotted lines, $d_{H-N} = 2.89$ Å). The interatomic distances between two superposed aromatic cycles are superior at 3.5 Å. The shortest distance of 3.46 Å is observed between the oxygen and carbon atoms of benzofuran cycles (blue dotted line in Figure 3B). Many lateral interactions take place between molecules of the adjacent columns, particularly through the benzofuran cycles which are placed opposite each other. Short oxygen – carbon distances of 3.27 Å (green dotted line in Figure 3B) are observed. Moreover, hydrogen bonds between hydrogen and oxygen atoms of benzofuran units (orange dotted lines, $d_{H-O} =$ 2.79 and 2.83 Å) reinforce the lateral contacts between the molecules. Finally, the many lateral contacts have tendency to compact the structure and it cannot be considered of true π-stacking in the packing mode of **Be3**. For the compound **Fu1** the cyanofuran moieties strongly participate in the intermolecular interactions. Firstly, **Fu1** co-crystallises with $CHCl_3$ molecule via the formation of hydrogen bonds ($d_{H-N} = 62$ Å, yellow dotted line in figure 3C) between the hydrogen of the solvent and the nitrogen atom of the cyano group grafted on furan unit. The molecules **Fu1** stack up along the *b* axis by deploying a strong π-π stacking mode characterized by numerous interatomic interactions with short distances less than 3.5 Å, as represented by blue dotted lines in figure 3C. Between adjacent columns, the hydrogen and nitrogen atoms of the cyanovinylene bonds are in intermolecular interactions by the existence of hydrogen bonds with $d_{H-N} = 2.47$ Å (orange dotted lines in figure 3C).

The compact structure of **Fu2** is obtained by the formation of columns of molecules stacking in two almost perpendicular directions as shown in figure 4A. In each column, the molecules stack with a slight shift such that the central furan cycle of a molecule between two cyanovynil bonds. The distances d separating two benzofuran planes are of 3.34 Å and the several short interatomic distances less than 3.4 Å involve the atoms of benzofuran, furan and cyanovinyl moieties. Thus this structure

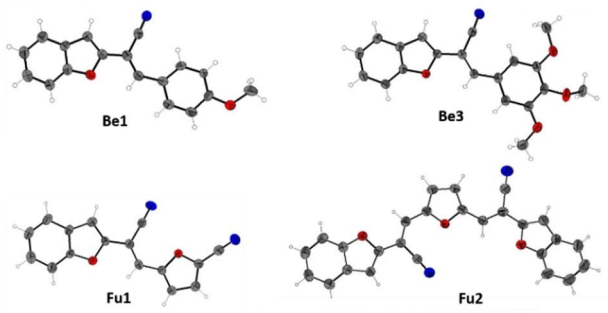

Figure 2. ORTEP views of compounds **Be1, Be3**, **Fu1** and **Fu2** showing their E-configuration.

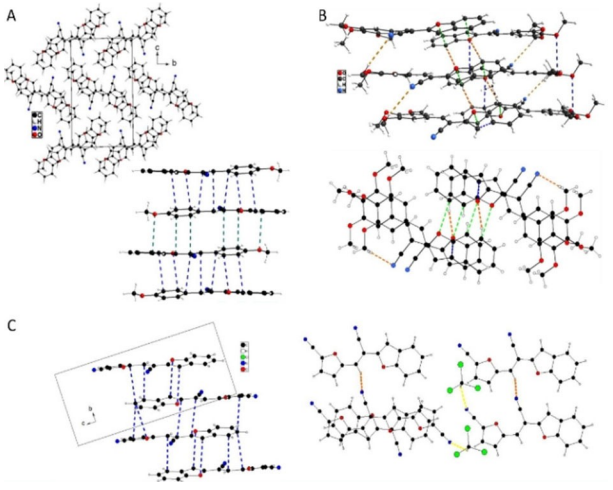

Figure 3. X-ray structures showing the molecular packing of **Be1** (A), **Be3** (B) and **Fu1** (C).

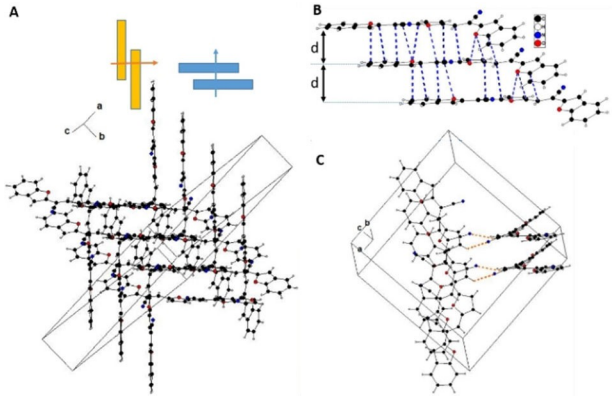

Figure 4. X-ray structure of compound **Fu2** showing the packing mode of the molecules in the crystal (A), the π-π stacking interactions in a column (B), the hydrogen bond contacts (orange dotted lines) between molecules of adjacent columns (C).

reveals the formation of strong π-π stacking in two perpendicular directions. Moreover, the nitrogen atoms of cyano groups induce interactions between adjacent columns of different orientation by hydrogen bonds with hydrogen of furan cycles ($d_{H-N} = 2.66$ Å, orange dotted lines in figure 4C).

The electronic properties of the molecules were evaluated by theoretical calculations and analysed by absorption and emission electronic spectroscopies and cyclic voltammetry.

Theoretical calculations were performed at the ab initio density functional level using the Gaussian09 package. Becke's three parameters gradient corrected functional (B3LYP) with a polarized 6-31G(d,p) was used for the geometrical optimization and for the HOMO and LUMO level determination. The E-configuration for the cyanovinyl units was used for the calculation for all the compounds. The theoretical data are gathered in Table 1. For the fully optimized geometries, the aromatic cycles and the vinylene bonds are found to be coplanar (Figure S2 in the Supporting Information). For the derivatives of the **Be** series, the methoxy groups of the 3 and 5 positions have little influence on the HOMO and LUMO levels. The HOMOs are delocalized along the conjugated systems whereas the LUMO are rather localized on the cyanovinyl bond. For the three molecules **Be1**-**Be3**, the band gap ΔE of the molecules are very close around 3.35 eV. In the furaldehyde series, for compound **Fu1**, the cyano group in 5-position of the furan causes a stabilisation both of the HOMO and LUMO levels leading to a decrease of the band gap up to 3.09 eV. The LUMO present a delocalization between the two cyano groups through the vinylene and furan units. Finally, for the more extended systems **Fu2**, the HOMO is delocalized along all the conjugated systems and the LUMO is more localized between the two cyano groups though the central furan cycle. The band gap of the molecule **Fu2** reaches a value of 2.47 eV.

The absorption and fluorescence properties of all the compounds were first evaluated in dilute (10^{-5} M) chloroform

Table 1. HOMO and LUMO energy levels, theoretical bandgap ΔE calculated by DFT methods.[a]

Compound	HOMO [eV]	LUMO [eV]	ΔE_{theo} [eV]
Be1	−5.45	−2.10	3.35
Be2	−5.44	−2.06	3.38
Be3	−5.44	−2.06	3.36
Fu1	−5.98	−2.89	3.09
Fu2	−5.45	−2.98	2.47

[a] (B3LYP) 6–31G(d,p).

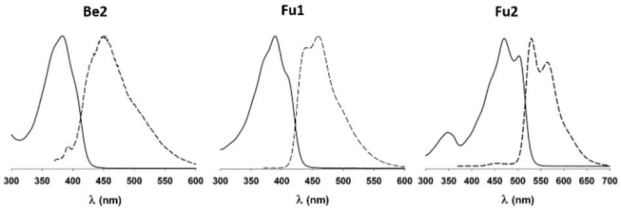

Figure 5. Normalized absorption (solid line) and emission (dashed line) spectra at 10^{-5} M in chloroform of **Be2**, **Fu1** and **Fu2**

to benchmark the properties and to ensure the absence of any supramolecular contacts and aggregates. Then the solid state emission properties were examined to evaluate the cyanovinylene mediated solid state emission enhancement. All the optical data in solution and in the solid state are gathered in table 2. The absorption and emission spectra of **Be2**, **Fu1** and **Fu2** are presented in Figure 5

The UV-Vis absorption spectra of compounds **Be1**–**Be3** present similar properties characterized by a slightly structured band with maxima at 378–383 nm (see figure 5 for **Be2**). The molecular absorption coefficients are superior at 35000 L mol^{-1}cm^{-1}. Under excitation at 350 nm, the emissions in solution are very low with a quantum yield Φ_{solu} inferior at 1%. The spectra present large unstructured band with maxima around 450 nm. The stokes shift for these compounds are close to 70 nm. These characteristics suggest non rigidified systems as often observed for cyanostilbene derivatives with the nitrile that enhances the rotational disorder of the aromatic neighbours. The non-radiative deactivation mode is efficient in solution resulting in supressed emission.[42] By contrast, the compounds **Fu1** and **Fu2** show very different behaviours in solution. For **Fu1** the absorption and emission bands present a net structuration with the presence of a shoulder for the UV-Vis and two maxima for the emission. Moreover, the stock shift decreases to 30 nm while the quantum yield Φ_{Sol} reaches up to 38%. Compound **Fu2** show a structured absorption band with two maxima at 470 and 502 nm. The fluorescence spectrum shows a fine vibronic structure with two maxima at 529 and 563 nm. The resulting orange red emission in chloroform has a quantum yield of 18%. By comparison, the analogue derivative in which the external benzofuran moieties are replaced by phenyl cycles,[43] presented unstructured absorption band while the emission in solution was quasi inexistent. Thus, the external benzofuran moieties lead to a rigidification of the extended

Table 2. Optical data of compounds, absorption and emission in solution and emission for the solid state.

Cpd	Solution λ_{max}[a] [nm]	ε [Lmol^{-1}cm^{-1}]	λ_{em}[a] [nm]	Δ_{Stokes} [nm]	Φ_{solu}[b] [%]	Solid λ_{em} [nm]	Φ_{soli}[b] [%]
Be1	348	35465	452	68	<1	512	<1
Be2	382	35665	451	69	<1	515	32
Be3	378	35490	452	74	<1	500	46
Fu1	389	36665	460	30	38	560	2
Fu2	470	50285	564	30	18	640	<1

[a] in $CHCl_3$ solution. [b] Absolute quantum yield.

conjugated systems favourable for the fluorescence emission in solution.

For the emission properties in the solid states, aggregates or crystals, opposite behaviours are observed between the **Be** and **Fu** series. The effect of formation of aggregates by increasing the quantity of water in THF-H_2O mixture are shown in figure 6 for **Be3**. Under excitation at 360 nm, the emission of **Be3** in THF solution is very low but strongly increases with the formation of aggregates in a mixture THF-water (15/85) to give a yellow emission (Figure 6A). Such net aggregation induced emission (AIE) effect[44] is also observed for **Be2**. Finally, the two compounds **Be2** and **Be3** show high green emission in the solid state both for powders and crystals with a fluorescence spectra characterized by large band with maxima at 515 nm for **Be2** and 500 nm for **Be3** (Figure 7B) and absolute quantum yields of 32% and 46% for **Be2** and **Be3**, respectively.

By contrast, **Be1** does not present any AIE effect and the quantum yield for the solid state is inferior at 1%. This difference of behaviour can be explained by comparing the stacking modes of **Be1** and **Be3** in the X-ray structures. The formation of π-dimers that are well known for quenching the emissive properties,[45,46] is clearly evidenced in the structure of **Be1** (Figure 3A). By contrast for **Be3**, no π-stacking is observed while many intermolecular contacts by hydrogen bonds are observed (Figure 3B). Such interactions in the aggregates allow the restriction of intramolecular rotation thus favouring the radiative decay pathway leading to high emissive solid.[47] On the other hand, the X-Ray diffraction of single crystals of **Be1** let under daylight for several hours shows the apparition of a new derivative in the solid. After 12 h of irradiation at 365 nm, the resolution of the structure indicates the presence of **Be1** and a cyclobutane derivative **Cy-Be1** statistically distributed at 55/45% in the crystal respectively (Figure 7A). **Cy-Be1** is obtained by [2+2] cycloaddition under irradiation at 365 nm between the two cyanovinyl bonds.[48,49,50] The cyclobutane **Cy-Be1** is only under a diastereroisomer form with the cyano groups in anti-position.[51] The analysis of the structure demonstrates that the π-dimers of **Be1** formed in a head-to-tail orientation presents the adequate approach with a distance d = 3.74 Å between centroids of the cyanovinyl bonds, according with the Schmidt rules to give the specific [2+2] cycloaddition.[52] It can be noted that the irradiation of crystals of **Be3** does not lead to structural evolution. When powders of **Be1**, **Be2** and **Be3** are irradiated at 365 nm during 12 h, the resulting ^{1}H NMR spectra in $CDCl_3$ of **Be2** and **Be3** do not present any evolution, while for **Be1**, new singlets appear at 5.33 ppm and 6.87 ppm and a doublet appears at 6.77 ppm (Figure 7B). Moreover, a new singlet appears at 3.72 ppm at side the singlet associated at the methoxy group at 3.9 ppm. Such evolution is characteristic of the formation of the compound **Cy-Be1**. Based on the integration of the singlets of methoxy groups, the rate of cyclobutane adduct **Cy-Be1** is evaluated at 45%. By increasing the time of irradiation at 24 h, the rate reaches about 85% and **Cy-Be1** can be easily isolated by flash chromatography.

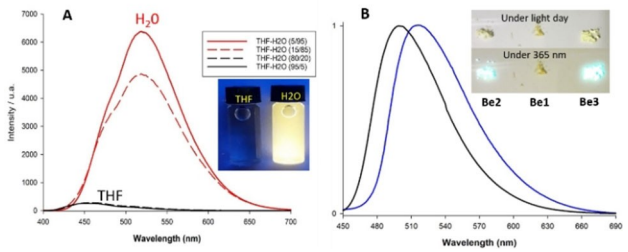

Figure 6. A) Emission spectra of **Be3** (10^{-5} M) in THF-H_2O mixture (black for THF/H_2O 95/5 and red for THF/H_2O 5/95), inset: photograph of **Be3** in THF and H_2O irradiated with UV lamp (365 nm). B) Normalized emission spectra of **Be2** (blue) and **Be3** (black) with excitation at 350 nm, inset: photograph of powders of **Be1**, **Be2**, **Be3** under daylight or UV (365 nm) light.

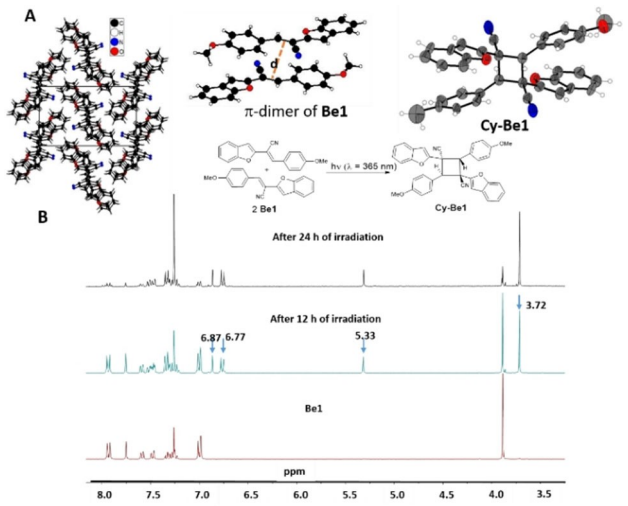

Figure 7. A) X-ray structure of the hybrid **Be1-CyBe1** crystals, π-dimers of **Be1** with the distance d between the centroids of the cyanovinyl bonds, Ortep view of cyclobutane derivatives **Cy-Be1**. B) ^{1}H NMR in $CDCl_3$ of **Be1** (bottom) then irradiated **Be1** with UV light (365 nm) for 12 h and 24 h, Scheme of the [2+2] cycloaddition.

Concerning the **Fu** series, the effect of addition of water in THF solution on the fluorescence is shown in figure 8. For **Fu1** (Figure 8A) the blue emission in the THF turns out to be improved by increasing the quantity of water in the solvent to reach a higher emission when the water proportion is 60%. Further increasing of the water proportion in the solvent results in the formation of aggregates which tend to decrease the emission property. At the end, the aggregates obtained in water have a low orange emission characterized by a wide

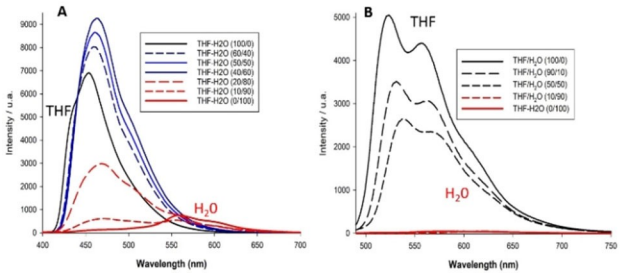

Figure 8. Fluorescence spectra of 10^{-5} M **Fu1** (A) and **Fu2** (B) as a function of THF/water (v/v) mixtures under excitation at 360 nm.

band with a maximum at 560 nm. The quantum yield of emission of **Fu1** in the solid state is only 2%. Finally, for **Fu2** (Figure 8B) a net aggregation caused quenching (ACQ) effect is observed with high orange- yellow emission in THF solution that decreases by increasing the quantity of water for quasi vanishing the emission when aggregates are formed. This ACQ effect for **Fu** series can be explained by the tendency of the molecules to create strong π-stacking, as observed in the X-ray structures.

The electrochemical properties of compounds were analysed using cyclic voltammetry at 10^{-3} mol L^{-1} in 0.1 M Bu_4NPF_6 CH_2Cl_2 solution (Figure 9) The electrochemical data gathering oxidation (E_{ox}) and reduction (E_{red}) potentials are given in Table 3. The derivatives of **Be** series present similar electrochemical behaviours characterized by an irreversible oxidation peak around 1.20–1.25 V and an irreversible reduction peak close to −1.85 V. The electrochemical gap calculated by the difference between the foot of the oxidation and reduction peaks are of 2.7 eV for **Be1** and 2.9 eV for **Be2** an **Be3**. The CV of **Fu1** also presents an irreversible oxidation peak but at higher potential of 1.4 V owing to the stabilization of the HOMO level provoked by the presence of the cyano group on the furan. In reduction, the electrochemical behaviour is modified with the apparition of two irreversible peaks at −1.39 and −1.71 V. As expected, the strong stabilization of the LUMO level allows the access to radical anion at higher potential but also the formation of dianion state. Finally, the oxidation of compound **Fu2** presents a broad irreversible oxidation wave with a potential peak at 1.56 V and a shoulder at 1.33 V. These two close oxidation processes correspond to the formation of radical cation then dication. The reduction processes are characterized by two reversible peaks at −1.19 and −1.45 V. The lengthening of the conjugated backbone and the presence of two cyanovinyl bonds favour the formation of multiple oxidized and reduced states.

Considering the electrochemical properties of **Fu2** and its tendency to form π-stacking in two opposite directions that are ideal aptitudes for the development of organic field-effect transistors. OFET devices based on **Fu2** were fabricated in a bottom contact geometry. A series of ten transistors have been done and all the devices showed only p-type behaviour characterized by the amplification mode *Id* when negative gate voltage Vg increased (Figure S3 in the Supporting Information). It can be noted that CV of film of **Fu2** on platinum disk presented a large and partially reversible oxidation wave with a peak potential at 1.45 V (see Figure S4), indicating the formation of stable positive charge carriers. Field effect mobility (μ), threshold voltage (Vth) and on/off ratio (Ion/Ioff) of the OFETs are indicated in Table 4. The upper carrier mobility value reaches 1.39 10^{-4} cm^2 V^{-1} s^{-1} with an average value of 8.37 10^{-5} cm^2 V^{-1} s^{-1} that corresponds to results obtained for small molecules based on benzodifuran moieties.[20,22,53]

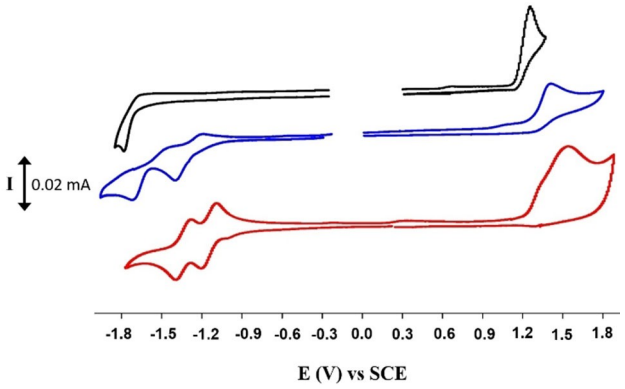

Figure 9. CVs of **Be1**, **Fu1** and **Fu2** 10^{-3} mol L^{-1} in 0.1 M Bu_4NPF_6 CH_2Cl_2, v = 100 mV s^{-1}.

Table 3. Electrochemical data of compounds.[a]

Compound	E_{ox} [V]	E_{red} [V]	ΔE_{elec} [eV][b]
Be1	1.20	−1.79	2.8
Be2	1.24	−1.81	2.9
Be3	1.25	−1.82	2.9
Fu1	1.40	−1.39	2.6
		−1.71	
Fu2	1.33	−1.19	2.3
	1.56	−1.45	

[a] 10^{-3} mol L^{-1} in 0.1 M Bu_4NPF_6 CH_2Cl_2, v = 100 mV s^{-1}, E versus SCE.

Conclusion

New extended benzofuran - aryl derivatives connected by cyano-vinylene junctions have been synthesized and their electronic properties investigated. The aryl cores derived from benzaldehyde or furaldehyde bio sourced platforms, induce net differences in the optical and electrochemical behaviours. Thus, for the emissive properties, methoxy phenyl derivatives present rather an AIE effect with higher solid – state emission than in solution. Nevertheless, as shown for less bulky derivative bearing only one methoxy group, the emission in the solid state can be annihilated when antiparallel π-dimers leads to cyclobutane derivatives through [2+2] cycloaddition when illuminated with 365 nm light. By contrast, the two derivatives with furan unit exhibit more rigidified extended systems giving higher fluorescence in solution than in solid state. Crystal

Table 4. Mobility, $V_{th,}$ and $I_{on/off}$ data obtained for transistors made from **Fu2**.

OFET number	Mobility [cm^2 V^{-1} s^{-1}]	V_{th} [V]	$I_{on/off}$
1	1.39 10^{-4}	−20	10^2
2	1.06 10^{-4}	−20	10^2
3	8.33 10^{-5}	−18	10^2
4	6.97 10^{-5}	−18	10^2
5	6.03 10^{-5}	−18	10^2
6	8.90 10^{-5}	−20	10^2
7	9.27 10^{-5}	−20	10^2
8	7.58 10^{-5}	−18	10^2
9	6.46 10^{-5}	−18	10^2
10	5.65 10^{-5}	−15	10^2

[b] Calculated from the difference between the foot of the oxidation and reduction peaks.

analyses show that the furan cores favour the formation of strong π-stacking that quenches the solid state emission. Finally, the lengthening of the extended systems with the presence of two cyanovinyl bonds, induces the formation of a 2D π-stacking favourable to the development of organic field effect transistors.

Experimental Section

Detailed protocols for the synthesis of 2-coumaranone, ylide **Y** and aldehydes **DFF** and **FuCN** are presented in the Supporting Information.

^{1}H NMR and ^{13}C NMR spectra were obtained at 300 and 75 MHz respectively with $CDCl_3$ as solvent and the ^{1}H and ^{13}C chemical shifts were determined by reference to residual non deuterated solvent resonances. Data are reported as follows: chemical shift in ppm (δ), multiplicity (s = singlet, d = doublet, t = triplet, m = multiplet), integration and coupling constant (Hz).

Synthesis of 2-(benzofuran-2-yl)acetonitrile (1)

To a solution of 2-coumaranone (500 mg, 3.73 mmol) in toluene (5 mL) was added ylide **Y** (1.13 g, 3.75 mmol). The mixture was irradiated in a CEM Discover microwave (300 W, 150 °C, 5 bars) for 15 min. The solvent was then evaporated and the residue was treated with 10 mL of methanol. The solid corresponding to insoluble part of oxide of triphenylphosphine was filtered and washed with 5 mL of methanol (830 mg, 2.98 mmol). The filtrate containing the target molecule **1** was evaporated and the residue was purified over silica gel (petroleum ether/ methylene chloride 2/8) to give a white solid (450 mg, 2.87 mmol, 77% yield). ^{1}H NMR ($CDCl_3$): 7.56 (dd, 1H, *J* = 7.3 Hz, *J* = 1.1 Hz), 7.46 (d, 1H, *J* = 7.9 Hz), 7.35-7.21 (m, 2H), 6.75 (d, 1H, *J* = 1.1 Hz), 3.92 (d, 2H, J = 1.1 Hz). ^{13}C NMR ($CDCl_3$): 155.4, 146.1, 127.9, 125.0, 123.4, 121.2, 115.1, 111.3, 105.6, 18.2. HRMS (EI) calculated for $C_{10}H_7NO$: 157.0528, found: 157.0525.

General Knoevenagel condensations procedure

A mixture of aldehyde (2 mmol), carbonitrile derivative **1** (2 mmol or 4 mmol) and catalytic amount of NaOtBu (10% mol) was stirred in ethanol (5 or 10 mL) for 12 h at room temperature. The resulting precipitate was filtered then washed with cold ethanol. Afterwards, the solid was dried in high *vacuo* to afford crystalline powders.

(E)-2-(benzofuran-2-yl)-3-(4-methoxyphenyl)acrylonitrile: Be1

Pale yellow solid (65% yield). ^{1}H NMR ($CDCl_3$): 7.93 (d, 2H, J = 8.7 Hz), 7.75 (s,1H), 7.58 (d, 1H, 7.7 Hz), 7.48 (d, 1H, 7.7 Hz), 7.32–7.23 (m, 2H), 7.00 (d, 2H, 8.7 Hz), 6.98 (s,1H), 3.89 (s, 3H). ^{13}C NMR ($CDCl_3$): 162.0, 155.2, 151.8, 140.0, 131.6, 128.8, 126.2, 125.5, 123.6, 121.6, 116.8, 114.7, 111.1, 105.6, 99.0, 55.6. HRMS (TOF) calculated for $C_{18}H_{13}NO_2$: 275.09408, found: 275.09403.

(E)-2-(benzofuran-2-yl)-3-(3,4-dimethoxyphenyl)acrylonitrile: Be2

Pale yellow solid (75% yield). ^{1}H NMR ($CDCl_3$):, 7.75 (s,1H), 7.72 (d, 1H, J = 2.2 Hz), 7.59 (d, 1H, 7.0 Hz), 7.48 (d, 1H, 7.6 Hz), 7.43 (dd, 1H, J = 8.4 Hz, J = 2.2 Hz), 7.36–7.23 (m, 2H), 7.00 (s,1H), 6.95 (d, 1H, J = 8.4 Hz), 3.99 and 3.96 (2 s, 6H). ^{13}C NMR ($CDCl_3$): 155.2, 151.7, 151.6, 149.2, 140.1, 128.6, 126.3, 125.5, 124.9, 123.5, 121.5, 116.8, 111.1, 111.0, 110.8, 105.5, 98.9, 64.1, 56.1. HRMS (TOF) calculated for $C_{19}H_{15}NO_3$: 305.1052, found: 305.10464.

(E)-2-(benzofuran-2-yl)-3-(3,4,5-trimethoxyphenyl) acrylonitrile: Be3

Yellow solid (70% yield). . ^{1}H NMR ($CDCl_3$):, 7.73 (s,1H), 7.61 (d, 1H, J = 7.1 Hz), 7.49 (d, 1H, 7.7 Hz), 7.37–7.27 (m, 2H), 7.24 (s,2H), 7.04 (s, 1H), 3.95 and 3.94 (2 s, 9H). ^{13}C NMR ($CDCl_3$): 155.3, 153.4, 151.3, 140.8, 140.1, 128.5, 125.7, 123.6, 121.6, 116.5, 111.1, 111.0, 106.9, 106.2, 100.5, 61.1, 56.2. HRMS (TOF) calculated for $C_{20}H_{17}NO_4$: 335.11521, found: 335.11495.

(E)-5-(2-(benzofuran-2-yl)-2-cyanovinyl)cyanofuran: Fu1

Orange solid (70% yield). ^{1}H NMR ($CDCl_3$):, 7.63 (d, 1H, J = 7.8 Hz), 7.58 (s,1H), 7.49 (d, 1H, 8.2 Hz), 7.41 (t, 1H, J = 7.2 Hz) 7.31 – 7.24 (m, 3H), 7.16 (s, 1H). ^{13}C NMR ($CDCl_3$): 155.7, 153.5, 149.8, 128.3, 127.3, 126.9, 124.0 (2), 123.6, 122.1, 114.8, 111.3, 110.9, 109.2, 103.2. HRMS (TOF) calculated for $C_{16}H_8N_2O_2$: 260.05913, found: 260.05856.

(2E,2′E)-3,3′-(furan-2,5-diyl)bis(2-(benzofuran-2-yl) acrylonitrile): Fu2

Red solid (75% yield). ^{1}H NMR ($CDCl_3$): 7.64 (s,1H), 7.60 (d, 1H, J = 7.7 Hz), 7.50 (d, 1H, 8.2 Hz), 7.39 (s, 1H), 7.40–7.25 (m, 2H), 7.11 (s, 1H). ^{13}C NMR ($CDCl_3$): 155.6, 151.9, 150.7, 128.5, 126.4, 124.2, 123.8, 121.8, 118.5, 115.6, 111.2, 107.9, 100.5. HRMS (TOF) calculated for $C_{26}H_{14}N_2O_3$: 402.09989, found: 402.10008.

Cycloaddition [2 + 2] (1R,2R,3S,4S)-1,3-di(benzofuran-2-yl)-2, 4-bis(4-methoxyphenyl)cyclobutane-1,3-dicarbonitrile: Cy-Be1

Ground powder of **Be1** (15 mg) was irradiated for 18–24 h with a 366 nm lamp (P = 10 W). The cycloaddition can be followed by TLC with eluent DCM/EP (1/1) with Rf = 0.8 for **Be1** and Rf = 0.2 for **Cy-Be1**. The resulting solid was dissolved in 1 mL of dichloromethane and chromatographed under silica gel (eluent DCM/EP 1/1) to separate **Be1** and **Cy-Be1**.

White solid (70% yield). ^{1}H NMR ($CDCl_3$): 7.56–7.48 (m, 4H), 7.38-7.24 (m, 8H), 6.90 (s, 2H), 6–78 (d, 4H, J = 8 Hz), 5,35 (s, 2H), 3.73 (s, 6H). ^{13}C NMR ($CDCl_3$): 160.1, 155.3, 149.3, 130.2,127.5,125.5,124.1, 123.6, 121.6, 118.9, 114.2, 111.7, 108.2, 55.3, 54.8, 45.3. HRMS (TOF) calculated for $C_{36}H_{26}N_2O_4Na$: 573.17848, found: 573.17992

X-ray crystallography

Single crystals suitable for X-ray diffraction analyses were obtained for all the compounds by the slow evaporation of ethanol – chloroform solution.

X-ray single-crystal diffraction data were collected on an a Rigaku Oxford Diffraction SuperNova diffractometer equipped with Atlas CCD detector and mirror monochromated micro-focus Cu-K_α radiation (λ = 1.54184 Å). The structures were solved by direct methods or dual-space algorithm (using ShelxS/ShelXT) and refined on F^2 by full matrix least-squares techniques using SHELX (G.M. Sheldrick, 1997, 2014, 2016, 2018) package. All non-hydrogen atoms were refined anisotropically and the H atoms were included in the calculation without refinement. Multiscan empirical absorption was corrected using CrysAlisPro program (CrysAlisPro, Agilent Technologies,/Rigaku Oxford Diffraction, 2014–2019).

The data collection details are gathered in Tables S1 and S2 in the Supporting Information.

Deposition Numbers 2059071 for **1**, 2059076 for **Be1**, 2059077 for **Be1**-**CyBe1**, 2059078 for **Be3**, 2059080 for **Fu1** and 2059081 for **Fu2** contain the supplementary crystallographic data for this paper. These data are provided free of charge by the joint Cambridge Crystallographic Data Centre and Fachinformationszentrum Karlsruhe Access Structures service www.ccdc.cam.ac.uk/structures.

Conflict of Interest

The authors declare no conflict of interest.

Keywords: benzofuran · conjugated materials · cyanostilbene · cycloaddition · emissive materials

[1] A. Corma, S. Iborra, A. Velty, *Chem. Rev.* **2007**, *107*, 2411–2502.
[2] Y. Liu, Y. Nie, X. Lu, X. Zhang, H. He, F. Pan, L. Zhou, X. Liu, X. Ji, S. Zhang, *Green Chem.* **2019**, *21*, 3499–3535.
[3] J. S. Mahajan, R. M. O'Dea, J. B. Norris, L. T. J. Korley, T. H. Epps, *ACS Sustainable Chem. Eng.* **2020**, *8*, 15072–15096.
[4] H. Ji, C. Dong, G. Yang, Z. Pang, *ACS Sustainable Chem. Eng.* **2018**, *6*, 15306–15315.
[5] B. Rajkumar, L. Khanam, E. N. Koukaras, G. D. Sharma, S. P. Singh, B. Lochab, *ACS Sustainable Chem. Eng.* **2020**, *8*, 5891–5902.
[6] O. Gidron, A. Dadvand, Y. Sheynin, M. Bendikov, D. F. Perepichka, *Chem. Commun.* **2011**, *47*, 1976–1978.
[7] S. Gillet, M. Aguedo, L. Petitjean, A. R. C. Morais, A. M. da Costa Lopes, R. M. Łukasik, P. T. Anastas, *Green Chem.* **2017**, *19*, 4200–4233.
[8] Z. Sun, B. Fridrich, A. de Santi, S. Elangovan, K. Barta, *Chem. Rev.* **2018**, *118*, 614–678.
[9] W. Schutyser, T. Renders, S. Van den Bosch, S. F. Koelewijn, G. T. Beckham, B. F. Sels, *Chem. Soc. Rev.* **2018**, *47*, 852–908.
[10] O. Y. Abdelaziz, C. P. Hulteberg, *ChemSusChem* **2020**, *13*, 4382–4384.
[11] R.-J. van Putten, J. C. van der Waal, E. de Jong, C. B. Rasrendra, H. J. Heeres, J. G. de Vries, *Chem. Rev.* **2013**, *113*, 1499–1597.
[12] F. A. Kucherov, L. V. Romashov, K. I. Galkin, V. P. Ananikov, *ACS Sustainable Chem. Eng.* **2018**, *6*, 8064–8092.
[13] Y. Peng, X. Li, T. Gao, T. Li, W. Yang, *Green Chem.* **2019**, *21*, 4169–4177.
[14] R. A. Sheldon, *Curr. Opin. Green Sustain. Chem.* **2018**, *14*, 89–95.
[15] P. Huang, J. Du, M. C. Biewer, M. C. Stefan, *J. Mater. Chem. A* **2015**, *3*, 6244–6257.
[16] A. Islam, Z.-y. Liu, R.-x. Peng, W.-g. Jiang, T. Lei, W. Li, L. Zhang, R.-j. Yang, Q. Guan, Z.-y. Ge, *Chin. J. Polym. Sci.* **2017**, *35*, 171–183.
[17] J. Du, C. Bulumulla, I. Mejia, G. T. McCandless, M. C. Biewer, M. C. Stefan, *Polym. Chem.* **2017**, *8*, 6181–6187.
[18] O. Gidron, M. Bendikov, *Angew. Chem. Int. Ed.* **2014**, *53*, 2546–2555; *Angew. Chem.* **2014**, *126*, 2580–2589.
[19] H. Cao, P. A. Rupar, *Chem. Eur. J.* **2017**, *23*, 14670–14675.
[20] C. Mallet, Y. Didane, T. Watanabe, N. Yoshimoto, M. Allain, C. Videlot-Ackermann, P. Frère, *ChemPlusChem* **2013**, *78*, 459–466.
[21] J.-X. Qiu, Y.-X. Li, J.-L. Miao, Z.-W. Zhang, Z.-H. Chen, *Synth. Met.* **2015**, *199*, 353–359.
[22] G. H. Rao, M. Pandey, K. Narayanaswamy, R. Srinivasa Rao, S. S. Pandey, S. Hayase, S. P. Singh, *ACS Omega* **2018**, *3*, 13919–13927.
[23] J. Grolleau, R. Petrov, M. Allain, W. G. Skene, P. Frère, *ACS Omega* **2018**, *3*, 18542–18552.
[24] J.-X. Qiu, Y.-X. Li, X.-F. Yang, Y. Nie, Z.-W. Zhang, Z.-H. Chen, G.-X. Sun, *J. Mater. Chem. C* **2014**, *2*, 5954–5962.
[25] H. Wang, C. Zhu, D. Li, Q. Liu, J. Tan, C. Wang, C. Cai, L. Ma, *Renewable Sustainable Energy Rev.* **2019**, *103*, 227–247.
[26] A. A. Rosatella, S. P. Simeonov, R. F. M. Frade, C. A. M. Afonso, *Green Chem.* **2011**, *13*, 754–793.
[27] C. Xu, E. Paone, D. Rodríguez-Padrón, R. Luque, F. Mauriello, *Chem. Soc. Rev.* **2020**, *49*, 4273–4306.
[28] X. Qi, M. Watanabe, T. M. Aida, J. R. L. Smith, *Green Chem.* **2009**, *11*, 1327–1331.
[29] C. Lansalot-Matras, C. Moreau, *Catal. Commun.* **2003**, *4*, 517–520.
[30] L. Lai, Y. Zhang, *ChemSusChem* **2011**, *4*, 1745–1748.
[31] A. Baliani, G. J. Bueno, M. L. Stewart, V. Yardley, R. Brun, M. P. Barrett, I. H. Gilbert, *J. Med. Chem.* **2005**, *48*, 5570–5579.
[32] M. Akira, O. Tetsuo, K. Seiichiro, *Bull. Chem. Soc. Jpn.* **1967**, *40*, 2875–2884.
[33] J. Ma, Z. Du, J. Xu, Q. Chu, Y. Pang, *ChemSusChem* **2011**, *4*, 51–54.
[34] M. Hong, J. Min, S. Wu, H. Cui, Y. Zhao, J. Li, S. Wang, *ACS Omega* **2019**, *4*, 7054–7060.
[35] P. Goncalo, C. Roussel, J. Marie Mélot, J. Vébrel, *J. Chem. Soc. Perkin Trans. 2* **1999**, 2111–2115.
[36] A. Faurie, F. Gohier, P. Frère, *Dyes Pigm.* **2018**, *154*, 38–43.
[37] M. Lakhrissi, Y. Chapleur, *Angew. Chem. Int. Ed.* **1996**, *35*, 750–752; *Angew. Chem.* **1996**, *108*, 833–834.
[38] G. Sabitha, M. M. Reddy, D. Srinivas, J. S. Yadov, *Tetrahedron Lett.* **1999**, *40*, 165–166.
[39] P. J. Murphy, S. E. Lee, *J. Chem. Soc. Perkin Trans. 1* **1999**, 3049–3066.
[40] E. Güllük, E. Bogdan, M. Christl, *Eur. J. Org. Chem.* **2006**, *2006*, 531–542.
[41] E. Podyacheva, E. Kuchuk, D. Chusov, *Tetrahedron Lett.* **2019**, *60*, 575–582.
[42] M. Martínez-Abadía, R. Giménez, M. B. Ros, *Adv. Mater.* **2018**, *30*, 1704161.
[43] C. Mallet, C. Moussallem, A. Faurie, M. Allain, F. Gohier, W. G. Skene, P. Frère, *Chem. Eur. J.* **2015**, *21*, 7944–7953.
[44] J. Mei, Y. Hong, J. W. Y. Lam, A. Qin, Y. Tang, B. Z. Tang, *Adv. Mater.* **2014**, *26*, 5429–5479.
[45] S. Varghese, S. Das, *J. Phys. Chem. Lett.* **2011**, *2*, 863–873.
[46] J. Gierschner, S. Y. Park, *J. Mater. Chem. C* **2013**, *1*, 5818–5832.
[47] J. Mei, N. L. C. Leung, R. T. K. Kwok, J. W. Y. Lam, B. Z. Tang, *Chem. Rev.* **2015**, *115*, 11718–11940.
[48] J. W. Chung, Y. You, H. S. Huh, B.-K. An, S.-J. Yoon, S. H. Kim, S. W. Lee, S. Y. Park, *J. Am. Chem. Soc.* **2009**, *131*, 8163–8172.
[49] S. Lin, K. G. Gutierrez-Cuevas, X. Zhang, J. Guo, Q. Li, *Adv. Funct. Mater.* **2020**, 2007957.
[50] E. Bosch, S. J. Kruse, E. W. Reinheimer, N. P. Rath, R. H. Groeneman, *CrystEngComm* **2019**, *21*, 6671–6675.
[51] S. Poplata, A. Tröster, Y.-Q. Zou, T. Bach, *Chem. Rev.* **2016**, *116*, 9748–9815.
[52] K. Biradha, R. Santra, *Chem. Soc. Rev.* **2013**, *42*, 950–967.
[53] B. Nketia-Yawson, H. Kang, E.-Y. Shin, Y. Xu, C. Yang, Y.-Y. Noh, *Org. Electron.* **2015**, *26*, 151–157.

Manuscript received: February 8, 2021
Revised manuscript received: February 26, 2021
Accepted manuscript online: March 1, 2021